OPEN ACCESS
IOP Publishing
Advances in Natural Sciences: Nanoscience and Nanotechnology
Adv. Nat. Sci.: Nanosci. Nanotechnol. **8** (2017) 015018 (6pp)
https://doi.org/10.1088/2043-6254/aa5957

Intrinsic phonon properties of double-walled carbon nanotubes*

H N Tran[1], D I Levshov[2], V C Nguyen[3], M Paillet[1], R Arenal[4,5], X T Than[1], A A Zahab[1], Y I Yuzyuk[2], N M Phan[3], J-L Sauvajol[1] and T Michel[1]

[1] Laboratoire Charles Coulomb, CNRS-University of Montpellier, CC069, 34095 Montpellier, France
[2] Faculty of Physics, Southern Federal University, 105/42 Bolshaya Sadovaya Str., Rostov-on-Don, 344006, Russia
[3] Institute of Materials Science, Vietnam Academy of Science and Technology, 18 Hoang Quoc Viet, Hanoi, Vietnam
[4] Laboratorio de Microscopías Avanzadas, Insituto de Nanociencia de Aragón, Universidad de Zaragoza, 50018 Zaragoza, Spain
[5] ARAID Foundation, 50018 Zaragoza, Spain

E-mail: Thierry.michel@umontpellier.fr

Received 9 November 2016
Accepted for publication 2 December 2016
Published 3 March 2017

Abstract

Double-walled carbon nanotubes (DWNT) are made of two concentric and weakly van der Waals coupled single-walled carbon nanotubes (SWNT). DWNTs are the simplest systems for studying the mechanical and electronic interactions between concentric carbon layers. In this paper we review recent results concerning the intrinsic features of phonons of DWNTs obtained from Raman experiments performed on index-identified DWNTs. The effect of the interlayer distance on the strength of the mechanical and electronic coupling between the layers, and thus on the frequencies of the Raman-active modes, namely the radial breathing-like modes (RBLMs) and G-modes, are evidenced and discussed.

Keywords: carbon nanotube, Raman spectroscopy, electron diffraction
Classification numbers: 2.00, 2.01, 5.14

1. Introduction

Individual carbon nanotubes (CNTs) are among the most promising materials for the modern photonics and optoelectronics [1]. High-resolution transmission electron microscopy (HRTEM) and electron diffraction (ED) are the most powerful methods for the determination of the structural parameters of individual CNTs, namely the number of walls and the chiral indices (n, m) of each layer which are directly related to its diameter and chiral angle. On the basis of this index-assignment resonant Raman spectroscopy (RRS) [2], absorption [3, 4] or Rayleigh spectroscopy [5, 6] allow to determine unambiguously the intrinsic optical and phonon properties of individual CNTs. Conversely, in some specific situations where ED fails to give unambiguous index-assignment of CNTs, Raman spectroscopy appears as a unique complementary tool for the index-assignment of the CNTs [7].

Double-walled carbon nanotubes (DWNTs) are made of two concentric and weakly van der Waals coupled single-walled carbon nanotubes (SWNTs). From a fundamental point of view, DWNTs are the simplest systems for studying the mechanical and electronic interactions between concentric carbon layers. On the other hand, DWNTs are emerging as promising SWNT substitutes as they exhibit higher stability and improved performances for several applications including optoelectronic and biosensors. Because a SWNT is uniquely characterized by its chiral indices (n, m), a DWNT is uniquely characterized by the chiral indices (n_i, m_i) and (n_o, m_o) of the constituent inner and outer SWNTs respectively, and the structure of a DWNT is identified as: (n_i, m_i)@(n_o, m_o). Because the inner and outer SWNTs can be either semiconducting (SC) or metallic (M), DWNTs display four different configurations: SC@SC, SC@M, M@SC and M@M,

* Invited talk at 8th International Workshop on Advanced Materials Science and Nanotechnology (IWAMSN2016), 8–12 November 2016, Ha Long City, Vietnam.

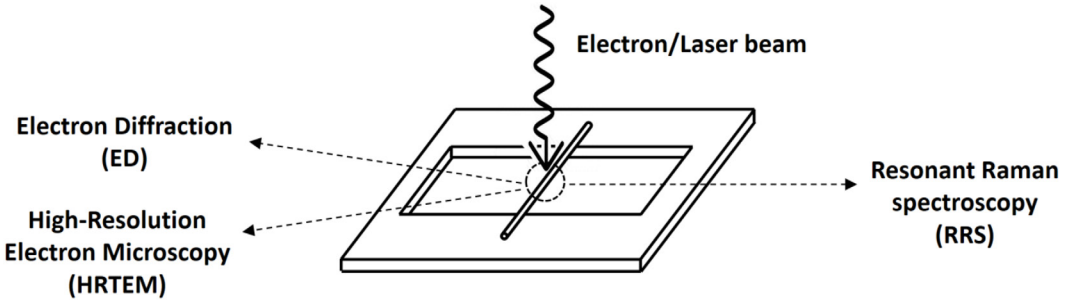

Figure 1. Illustration of the experimental design: individual free-standing (suspended) DWNTs are directly grown on commercial perforated silicon nitride TEM grids (hole diameters ~2 μm) or across home-made slits (slit width ~50 μm) on SiO_2/Si_xN_y substrates. This design enables the combination of HRTEM, ED, and Raman scattering (RRS) to, respectively, probe the structural and phonon properties of the same individual DWNT.

which possess distinct electronic properties. All the properties of DWNTs are related to the individual nature of the layers and their interactions. Especially, the wall-to-wall distance, which typically ranges from 0.3 nm to 0.38 nm, can affect the behavior of DWNT by changing the strength of the wall-to-wall interactions.

In this paper we report recent results obtained by combining HRTEM, ED and RRS experiments on individual free-standing index-identified DWNTs. By this way, intrinsic features of phonons of DWNTs are evidenced. We focus on the dependence of these features on the wall-to-wall distance.

2. Experimental

Ultra-long individual DWNT were grown by the catalytic chemical vapor deposition (CCVD) method directly on the commercial perforated silicon nitride TEM grids (hole diameters ~2 μm) or across home-made slits (slit width ~50 μm) fabricated by wet-etching of a Si_xN_y/Si wafers (for details, see [8]).

HRTEM and nano-beam ED experiments were performed in a FEI titan cubed C_s corrected 60–300 kV TEM operating at 80 kV. The DWNTs electron diffraction patterns (EDP) were recorded using a charge-coupled device (CCD) camera (Gatan Ultrascan 2 K × 2 K). The acquisition time of each EDP was <10 s. We have checked that with this procedure several EDPs can be acquired without any radiation damage of the tube.

RRS measurements were performed on a Jobin-Yvon iHR550 spectrometer (gratings 1800 or 1200 grooves per mm, precision $\approx\pm1\,cm^{-1}$) or a Jobin Yvon T64000 both equipped with a liquid-nitrogen-cooled, back-illuminated silicon CCD detector in a micro-Raman backscattering configuration (objective 100×, N.A. 0.95). Ar+, Kr+ lasers and tunable Ti:sapphire and dye lasers were used for excitation. In all experiments, incident and scattered light polarizations were oriented along the individual nanotubes axis (the so-called // // geometry). The laser power was always carefully controlled to avoid heating of the DWNTs. Figure 1 displays a sketch of the combined HRTEM, ED and RRS measurements performed on the same suspended DWNT.

3. Results

3.1. Raman spectroscopy of individual index-identified DWNTs

The low- and high frequency range of a Raman spectrum measured on the individual (16,12)@(27,10) DWNT is shown on figure 2. As expected with regards to the resonance conditions of the layers, the Raman spectrum significantly depends on the excitation energy. At several excitation energies, two modes are observed in the low-frequency range. They were assigned to in-phase and out-of-phase collective radial breathing vibrations of the constituent SWNT layers and called radial breathing-like modes (RBLMs) [9]. In the G modes range of this DWNT three components are clearly identified. Afterward, we detail the dependence of the two ranges of the Raman spectrum as a function of wall-to-wall distance and electronic configuration of the DWNT.

3.1.1. The collective RBLMs. The RBLM frequencies depend on the diameter of the constituent layers and on the mechanical coupling between the inner and outer layers [9]. It was shown experimentally that an up-shift of both in-phase and out-of-phase RBLM frequencies in comparison with the RBM frequencies of related individual SWNTs is observed [10, 11]. It was also experimentally established that the amplitude of the upshift depends on the inter-layer distance between concentric layers [11, 12].

In order to understand these results, different models of van-der-Walls coupled harmonic oscillators were developed in order to predict the dependence of the RBLM frequencies on the diameters of the inner and outer layers, associated to a given wall-to-wall distance [11, 13, 14]. In the simplest approach (see Liu *et al* [11]), the frequencies of the in-phase (ω_L) and out-of-phase (ω_H) RBLMs are given by

$$\omega_L = \frac{1}{2\pi c}\omega_c \sqrt{\frac{1}{2}\left[(z_1+z_2) - \sqrt{(z_1-z_2)^2+4}\right]}, \quad (1)$$

$$\omega_H = \frac{1}{2\pi c}\omega_c \sqrt{\frac{1}{2}\left[(z_1+z_2) + \sqrt{(z_1-z_2)^2+4}\right]}, \quad (2)$$

where $\omega_i^2 = \frac{k_i}{m_i}$, $\omega_o^2 = \frac{k_o}{m_o}$, $\omega_c^2 = \frac{k_c}{\sqrt{m_i m_o}}$, $z_1 = \frac{\omega_i^2}{\omega_c^2} + \sqrt{\frac{m_o}{m_i}}$ and $z_2 = \frac{\omega_o^2}{\omega_c^2} + \sqrt{\frac{m_i}{m_o}}$, m_i (m_o) are inner-wall (outer-wall) unit-length mass of the constituent SWNT and they are determined from the knowledge of the diameters of inner and outer SWNTs which are directly related to their chiral indices (n_i, m_i) and (n_o, m_o), respectively [11].

The intrinsic force constant k_i (k_o) for inner (outer) constituent SWNT can be accurately determined from the individual

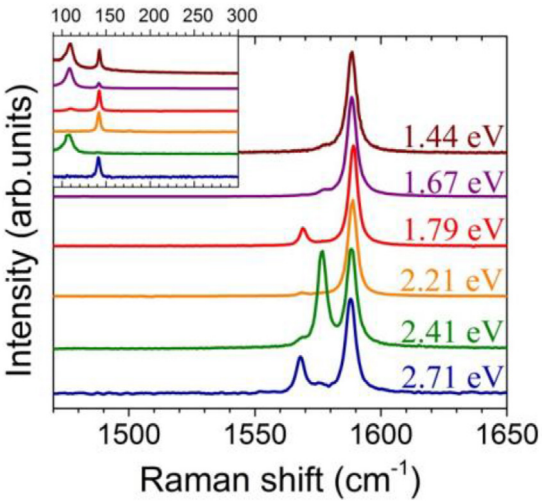

Figure 2. The low- (inset) and high frequency range of the Raman spectra measured on the individual (16,12)@(27,10) DWNT at the different excitation energies labelled on the right hand side.

radial breathing mode (RBM) frequency-diameter relationship [15]. It should be emphasized that we have to use the RBM frequency-diameter relations adapted to the experimental environment of each layer. In our experimental conditions (DWNT in air and room temperature), the frequencies of the RBM of the inner tube is given by $\omega_i = 228/d_i$ (nm) and that of the outer tube by $\omega_o = 228$ (cm^{-1} nm) $/d_o\ (1 + C_e d_o^2)^{1/2}$, with $C_e = 0.065\,\text{nm}^{-2}$ arising from the interaction of the outer-wall with the ambient atmosphere. The unit-length coupling force constant, k_c, characterizes the van-der-Waals interaction between the two concentric carbon nanotube layers. It can be approximated using the average unit-area inter-layer van-der-Waals potential U_{vdw} as

$$k_c = \frac{\partial^2 U_{vdw}}{\partial r^2}\pi\frac{(d_o + d_i)}{2}, \qquad (3)$$

where $(\partial^2 U_{vdw}/\partial r^2)$ is the unit-area force constant between the layers. The dependence of the unit-area force constant $(\partial^2 U_{vdw}/\partial r^2)$ on the inter-walls distance, δr, was recently established from measurements on index-identified DWNTs (see figure 3(d) of reference [11]). Therefore given wall-to-wall distance, δr, accurately derived from the assignment of the DWNT, one can use the figure 3(d) of reference [11] to estimate the value of $(\partial^2 U_{vdw}/\partial r^2)$, and then k_c, for each index-identified DWNT.

Using the previous expressions, we plot in figure 3 the calculated RBLM frequencies as a function of the diameter of inner (outer) nanotubes for wall-to-wall distance, $\delta r = \Delta D/2$, ranging from 0.32 to 0.38 nm. As expected, (i) RBLM are upshifted with respect to the RBM of the constituent SWNT, (ii) the RBLM frequencies decrease with increasing diameter of inner (outer) tubes, (iii) for the same inner (or outer) diameter, the RBLMs strongly depend on the wall-to-wall distance.

Figure 4 summarizes the experimental dependence of the RBLMs recently obtained from Raman experiments performed on several index-identified DWNTs.

It is confirmed that RBLM are upshifted with respect to the RBM of the constituent SWNT (the values of the shifts are given in parentheses in the figure 4). On the other hand, we clearly observe that: (i) for close inter-layer distance, both RBLM downshift when the tube diameters increase (figure 4, vertical arrow); (ii) for close average tube diameters and an interlayer distance δr larger than 0.335 nm (close to the equilibrium distance in graphite: 0.34 nm), the out-of-phase RBLM downshifts when the interlayer distance increases (figure 4, horizontal arrow). Both behaviors are in good agreement with the prediction of our simple model (see figure 3). As shown recently [11, 16], a given value of δr can be associated to an effective pressure between the layers: an interlayer distance larger (smaller) than 0.34 nm leads to an effective negative (positive) pressure between the layers. Negative (positive) pressure means that the inner-outer interaction causes a slight contraction (expansion) of the outer tube concomitant with the expansion (contraction) of the inner tube [11, 16]. In other words, the dependence of the shift of the RBLM on δr can be understood as a dependence on the effective pressure between the layers. It should be emphasized that the effective pressure (positive or negative) between the tubes reaches gigapascals owing to variations in the wall-to-wall distance [11]. Note that a negative pressure in the gigapascal range is difficult to achieve using conventional approaches.

3.1.2. The G modes. On the basis of the results established from Raman experiments performed on individual index-identified SWNTs [7], one expects to observe, in the range of the G modes, 4 (chiral@chiral), 3 (chiral@achiral or achiral@chiral) or 2 (achiral@achiral) components in the (// //) polarized Raman spectrum measured on an individual DWNT. Each component is assigned to the G^+ or G^- component of the coupled inner and outer constituent SWNTs. We remind that the G^+ component is assigned to the LO (TO) G mode and the G^- component to the TO (LO) G mode in SC (M) SWNT [7, 17]. However, in DWNTs, some components can appear at close frequencies and thus cannot be experimentally resolved.

Figure 5 compares the profile of G modes measured on index-identified SC@SC, M@SC, and SC@M DWNTs. We clearly establish that, as in SWNTs, the profile of the G^- component of each layer is broad (narrow) when the layer is metallic (SC) (figure 5, vertical direction). As a consequence, in terms of characterization, the observation of a broad component unambiguously identifies the presence of a metallic nanotube within the DWNT.

Recently the dependence of the G-modes frequencies on the diameter and inter-layer distance in SC@SC DWNT was reported [18]. It was found that the TO (G^- component) and LO (G^+ component) frequencies of the inner and outer tubes shift significantly in SC DWNTs with respect to the frequencies of the same modes in each constituent SWNT. Such dependence is illustrated on figure 5 (horizontal direction). The direction and values of the shift depend on the inter-layer distance [18]. Especially, as shown in figure 5 (inset), the shift of the G modes of the inner layer with respect to the G modes

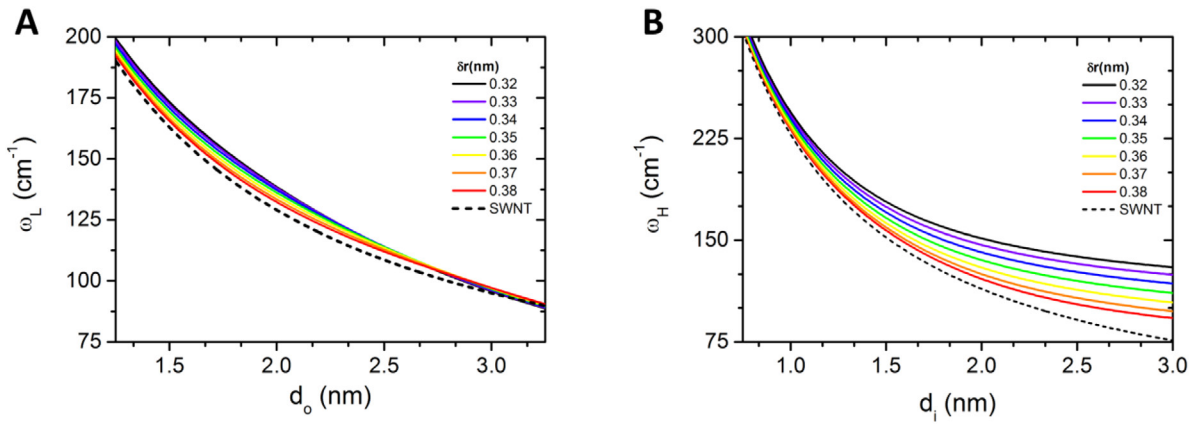

Figure 3. Frequencies of the in-phase (low-frequency, ω_L) and out-of-phase (high-frequency, ω_H) RBLMs as function of the diameter of the inner tube (a) and outer tube (b) for wall-to-wall distance $\delta r = \Delta D/2$ ranging from 0.32 to 0.38 nm.

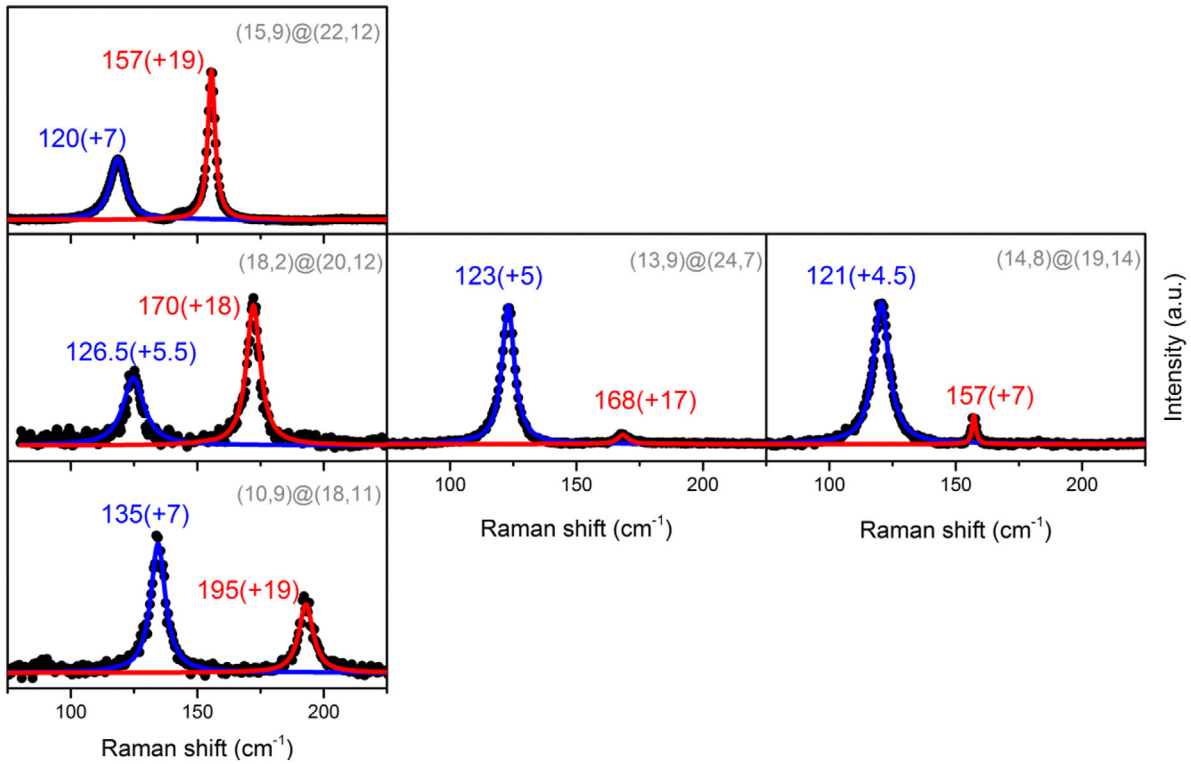

Figure 4. (vertical direction) Diameter dependence of the RBLM for DWNT with close inter-layer distances: top—(15,9)@(22,12) ($\langle d\rangle = (d_o + d_i)/2 = 1.992$ nm, and $\delta r = 0.348$ nm), middle—(18,2)@(20,12) ($\langle d\rangle = 1.843$ nm, and $\delta r = 0.349$ nm), bottom—(10,9)@(18,11) ($\langle d\rangle = 1.637$ nm, and $\delta r = 0.348$ nm); (horizontal direction) inter-layer distance dependence of the RBLM for DWNT with close average diameters: middle—(13,9)@(24,7) ($\langle d\rangle = 1.854$ nm, and $\delta r = 0.353$ nm), right—(14,8)@(19,14) ($\langle d\rangle = 1.879$ nm, and $\delta r = 0.368$ nm). The shifts of the RBLM with respect to the RBM frequencies of constituent SWNT are given in parentheses.

of the related SWNT increases with the inter-layer distance. We unambiguously establish that the larger the interlayer distance is, the larger is the shift of the LO and TO modes. As for RBLM, this shift is due to the negative effective pressure experienced by the inner and outer nanotube which occurs when the inter-layer distance is larger than the equilibrium distance evaluated at 0.335 nm in DWNT (close to the inter-layer distance in graphite, 0.34 nm).

In figure 6 we plot together the frequencies of the TO G-mode of the inner tube measured on index-identified DWNT (blue symbols) and, on the other hand, the ones obtained on (6,5)@SC DWNTs by Villalpando-Paez *et al* (red symbols) [19]. It must be emphasized that the index-assignment of the outer tubes of these later DWNTs, and then their δr values, was reexamined by comparing the experimental RBLMs of reference [19] with the results of the model presented in the previous subsection of this paper. A shift of the TO mode is observed in a large interlayer distance range. An upshift is found for δr smaller than 0.335 nm (positive pressure effect) and a downshift for δr larger than 0.335 nm (negative pressure effect). Theoretical calculations are in progress to relate these shifts to the amplitude of the effective pressure due to the structural relaxation (contraction or expansion) of the layers and including the interaction of the relaxed layers [20].

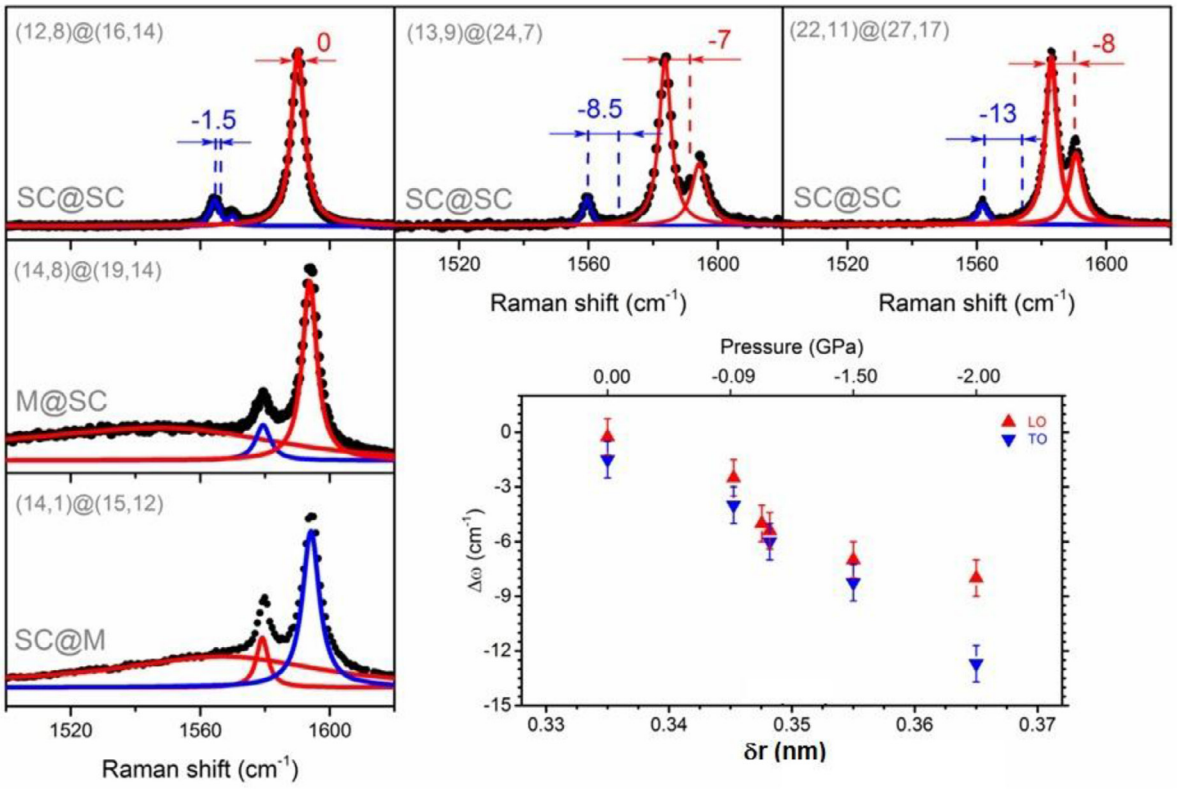

Figure 5. (vertical direction) The dependence of the G modes on the electronic configuration of DWNT: top—(12,8)@(16,14) (SC)@(SC), middle—(14,8)@(19,14) (M)@(SC), bottom—(14,1)@(15,12) (SC)@(M); (horizontal direction) the dependence of the G modes on the inter-layer distance δr: middle—(13,9)@(24,7), right—(22,11)@(27,17). The shifts of the G modes of the inner tube with respect to the G modes of the related individual SWNTs are given for the three SC DWNTs (dashed vertical lines). Inset: The dependence $\Delta\omega = \omega_{\mathrm{TO(DWNT)}} - \omega_{\mathrm{TO(SWNT)}}$ on δr.

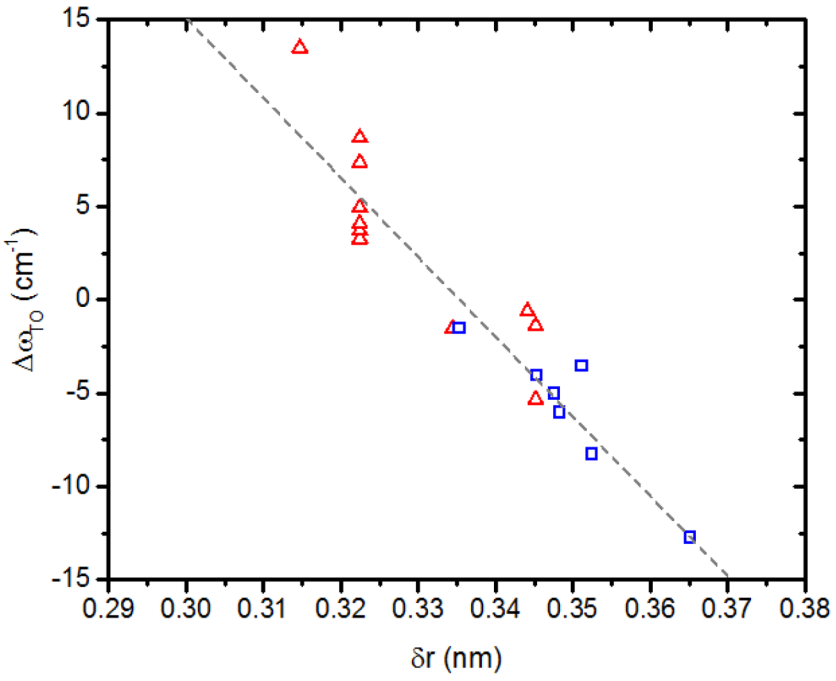

Figure 6. The TO frequencies shift, $\Delta\omega_{\mathrm{TO}} = \omega_{\mathrm{TO(DWNT)}} - \omega_{\mathrm{TO(SWNT)}}$, of the inner tube as a function of the inter-tubes distance. The blue open squares correspond to results obtained in index-identified individual suspended DWNTs (this work). The red open triangles correspond to data from reference [19] for (6,5)@(n_o,m_o) DWNTs with inter-tube distances reevaluated using the coupled oscillator mode ([11] and see text). The dashed line is a guide for eyes.

4. Conclusion

By combining HRTEM, ED, and RRS on individual, spatially isolated, and suspended DWNTs, we have been able to investigate in detail the dependence of the RBM and G-modes as a function of the structural parameters of index-identified DWNTs. We confirm that RBLM are upshifted with respect to the RBM of the constituent SWNT, and we clearly establish that: (i) for close inter-layer distance, both RBLM downshift when the tube diameters increase, (ii) for close average tube diameters and an interlayer distance δr larger than 0.335 nm, the out-of-phase RBLM downshifts when the interlayer distance increases. Concerning the G-modes, from the comparison of the profiles of G modes measured on index-identified SC@SC, M@SC, and SC@M DWNTs, we clearly establish that, as in SWNTs, the profile of the G^- component of each layer is broad (narrow) when the tube is metallic (SC). We unambiguously established the dependence of the frequencies of the G-modes on the distance between the inner and outer layers in SC@SC DWNTs: when the interlayer distance is larger (respectively smaller) than the nominal van der Waals distance (close to 0.335 nm), a downshift (respectively upshift) of the inner-layer G-modes with respect to the corresponding modes in equivalent SWNTs is measured, and larger (respectively smaller) is the interlayer distance, larger is the downshift (respectively upshift) of the LO and TO G-modes. The behaviors of the RBLM and G-modes as a function of the interlayer distance are well understood by considering the effect of an effective pressure felt by the inner and outer layers. These results emphasize the importance to study individual index-identified carbon nanotubes for a detailed understanding of all their intrinsic properties.

Acknowledgments

The authors thank V N Popov for discussions. VCN, NMP, HNT, MP and JLS acknowledge financial support by the International project of Scientific Cooperation with Vietnam (CNRS PICS 6457). NT, MP, AAZ and JLS acknowledge financial support by the ANR GAMBIT project grant ANR-13-BS10-0014 of the French Agence Nationale de la Recherche. DL gratefully acknowledges financial support of Russian Science Foundation (grant number 15-12-10004) and from RFBR Grant 15-12-08340. The TEM studies were conducted at the Laboratorio de Microscopías Avanzadas (LMA), Instituto de Nanociencia de Aragón (INA), Universidad de Zaragoza, Spain. Some of the research leading to these results has received funding from the European Union Seventh Framework Programme under Grant Agreements 312483-ESTEEM2 (Integrated Infrastructure Initiative - I3). RA gratefully acknowledges the support from the Spanish Ministry of Economy and Competitiveness (MINECO) through project grant FIS2013-46159-C3-3-P, from the Government of Aragon and the European Social Fund under the project "Construyendo Europa desde Aragon" 2014-2020 (grant number E/26), and from the European Union H2020 program under the ETN project Grant Agreement 642742.

References

[1] De Volder M, Tawfick S, Baughman R and Hart J 2013 *Science* **339** 535
[2] Meyer J, Paillet M, Michel T, Moréac A, Neumann A, Duesberg G S, Roth S and Sauvajol J L 2005 *Phys. Rev. Lett.* **95** 217401
[3] Blancon J-C *et al* 2013 *Nat. Commun.* **4** 2542
[4] Liu K, Jin C, Hong X, Kim J, Zettl A, Wang E and Wang F 2014 *Nat. Phys.* **10** 737
[5] Sfeir M Y *et al* 2006 *Science* **312** 554
[6] Berciaud S, Voisin C, Yan H, Chandra B, Caldwell R, Shan Y, Brus L E, Hone J and Heinz T F 2010 *Phys. Rev.* B **81** 041414
[7] Michel T, Paillet M, Nakabayashi D, Picher M, Jourdain V, Meyer J C, Zahb A A and Sauvajol J L 2009 *Phys. Rev.* B **80** 245416
[8] Than T X, Nguyen V C, Jourdain V, Paillet M, Kim D Y, Sauvajol J-L, Ngo T T T and Phan N M 2011 *J. Exp. Nanosci.* **6** 547
[9] Popov V N and Henrard L 2002 *Phys. Rev.* B **65** 235415
[10] Levshov D *et al* 2011 *Nano Lett.* **11** 4800
[11] Liu K *et al* 2013 *Nat. Commun.* **4** 1375
[12] Pfeiffer R, Simon F, Kuzmany H and Popov V N 2005 *Phys. Rev.* B **72** 161404
[13] Dobardzic E, Maultzsch J, Milosevic I, Thomsen C and Damnjanovic M 2003 *Phys. Status Solidi* b **237** R7
[14] Levshov D I *et al* 2016 *J. Nanophotonics* **10** 012502
[15] Araujo P T *et al* 2008 *Phys. Rev.* B **77** 241403
[16] Christofilos D, Arvanitidis J, Kourouklis G A, Ves S, Tanekobu T, Iwasa Y and Kataura H 2007 *Phys. Rev.* B **76** 113402
[17] Piscanec S, Lazzeri M, Robertson J, Ferrari A C and Mauri F 2007 *Phys Rev.* B **75** 035427
[18] Levshov D I, Michel T, Arenal R, Tran H N, Than T X, Paillet M, Yuzyuk Y I and Sauvajol J L 2015 *J. Phys. Chem.* C **119** 23196
[19] Villalpando-Paez F, Muramatsu H, Kim Y A, Farhat H, Endo M, Terrones M and Dresselhaus M S 2010 *Nanoscale* **2** 406
[20] Popov V N 2016 private communication